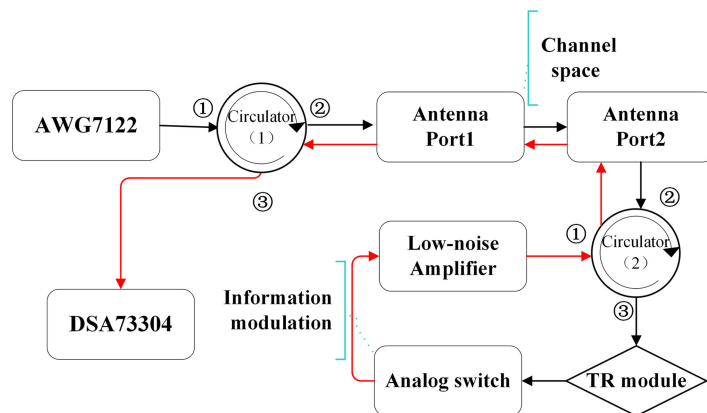


# Full Analog Broadband Time-Reversal Module for Ultra-Wideband Communication System

Volume 11, Number 5, October 2019

Zhipeng Wang  
Bing-Zhong Wang, *Senior Member, IEEE*  
Deshuang Zhao, *Member, IEEE*  
Ren Wang



DOI: 10.1109/JPHOT.2019.2936501

# Full Analog Broadband Time-Reversal Module for Ultra-Wideband Communication System

Zhipeng Wang , Bing-Zhong Wang , *Senior Member, IEEE*,  
Deshuang Zhao , *Member, IEEE*, and Ren Wang 

Institute of Applied Physics, University of Electronic Science and Technology of China,  
Chengdu 610054, China

DOI:10.1109/JPHOT.2019.2936501

This work is licensed under a Creative Commons Attribution 4.0 License. For more information, see  
<https://creativecommons.org/licenses/by/4.0/>

Manuscript received March 20, 2019; revised August 8, 2019; accepted August 16, 2019. Date of publication August 21, 2019; date of current version August 30, 2019. This work was supported in part by the National Natural Science Foundation of China under Grant 61331007, Grant 61601087, and Grant 61671133; in part by the Postdoctoral Innovation Talents Support Program under Grant BX20180057; and in part by the China Postdoctoral Science Foundation funded project under Grant 2018M640907. Corresponding author: Zhipeng Wang (e-mail: zpwanguestc@gmail.com).

**Abstract:** We built a full analog broadband time-reversal module and applied it to a prototype of ultra-wideband communication system. The time-reversal module is a temporal pulse shaping system using microwave photonic technology and it performs time-reversal operation on microwave signals based on the principle of temporal imaging. The module has an excellent time-reversal performance for microwave pulse signals and its system bandwidth exceeds 10 GHz. Based on the analog time-reversal module, a prototype of ultra-wideband communication system was established and we successfully completed the information transmission experiment to verify the feasibility of the system.

**Index Terms:** Time-reversal, Temporal pulse shaping, Microwave photonic technology, Ultra-wideband communication.

## 1. Introduction

Ultra-Wideband (UWB) communication has the advantages of relatively high penetration capability and high data rate in short-range wireless communication applications [1], [2]. However, there is a serious multipath delay interference effect in the indoor communication environment, which causes an increase in the communication error rate and reduces the information transfer rate. Based on the temporal-spatial focusing characteristics of time-reversal (TR) electromagnetic waves, the TR of microwave signals was proposed to overcome the multipath problem [3]. Based on this characteristic, TR technique was widely used in UWB communication system and experimental results have shown that the method is more reliable than traditional RAKE receiver in complex environment with rich multipath [4], and is conducive to improving data transmission rate and stability in a harsh wireless communication environment [5]–[8]. In addition, TR techniques have also been widely used for UWB remote sensing [9].

In TR-UWB communication systems, TR operation of microwave signals is an essential step, which can be divided into two categories: one based on digital signal processing technology and the other based on analog signal processing technology. The former method can directly sample, store and reverse the temporal signal; or temporal signal TR operation is realized by Fourier

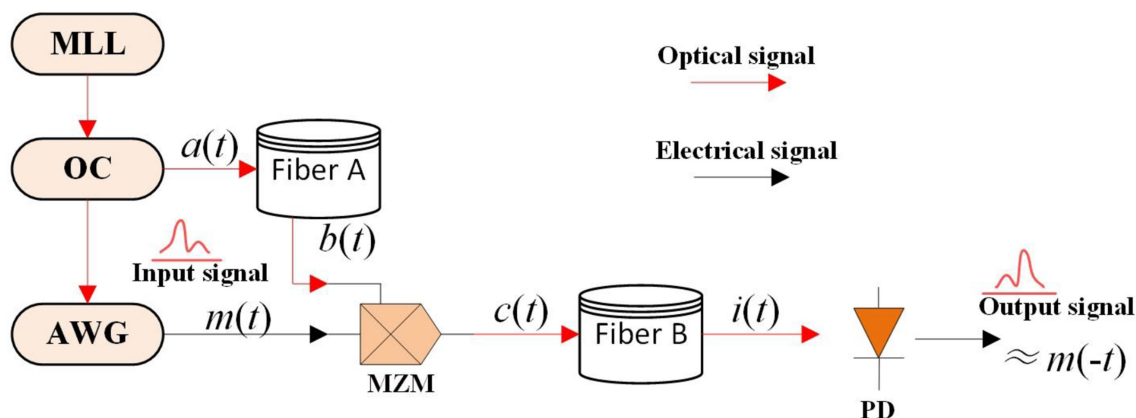


Fig. 1. Structure schematic of the time-reversal module based on microwave photonic technology. AWG: arbitrary waveform generator; OC: optical coupler MLL; mode-locked laser; MZM: Mach-Zehnder modulator; PD: photodetector.

transform and frequency domain phase conjugate. The inversion of the signal in the time domain is equivalent to phase conjugate transformation of each frequency component in the frequency domain [10]–[12]. Therefore, the temporal signal is transformed into the frequency domain by Fourier transform, the phase conjugate processing is performed on the signal in the frequency domain, and the TR signal can be obtained by inverse Fourier transform [13], [14]. The above analog methods cannot handle general aperiodic signals, and have poor real-time performance. Some scholars proposed TR operation of microwave signals according to the principle of temporal imaging [15], [16] which can be realized by analog signal processing technology, such as full electronic technology [17]–[19] and microwave photonic technology [20]–[22]. However, the limitations of the bandwidth, cost, and experimental conditions of the analog TR system make it difficult to apply to UWB communication systems, so that the TR operation of microwave signals in the TR-UWB communication system has been mostly realized by digital signal processing technology [5]–[8], which makes it necessary to rely on high-end experimental equipment and causes the code modulation and transmission of the information not to be performed in real time. The price of high-end analog to digital equipment used in the method has made the TR-UWB system only used for laboratory research, and it is hard to get into practical use.

Compared with full electronic technology, the TR system using microwave photonic technology has the advantages of high time-bandwidth product and high accuracy. This paper focus on building a broadband TR module based on microwave photonic technology. In this contribution, we built a low-cost broadband TR module and proposed a method of TR-UWB communication system using full analog devices. It not only used the analog signal processing technology instead of the digital signal processing technology in the microwave signal TR operation, but also used the analog device to encode and modulate the information in real time during the information transmission process.

## 2. Analog Time-Reversal Module

### 2.1 System Structure

The proposed microwave photonic TR module is shown in Fig. 1. A femtosecond optical pulse emitted by a mode-locked laser (MLL) is transmitted respectively to dispersion Fiber A and a photoelectric detector (PD) through a 90:10 optical coupler (OC). The output signal of the PD is used as a trigger signal of the arbitrary waveform generator (AWG). Therefore, the AWG generates a synchronous microwave signal,  $m(t)$ , which is applied to a Mach-Zehnder modulator (MZM). At the other port of the OC, the optical pulse  $a(t)$  is temporally broadened by Fiber A. The optical input port of the MZM is connected to Fiber A. Hence, the microwave signal to be reversed modulates

the optical signal by the MZM. The modulated optical pulse output from MZM,  $c(t)$ , is time-reversed by Fiber B. The envelope of the optical signal,  $i(t)$ , is finally detected by the PD connected to Fiber B and a TR microwave waveform is observed by real-time electronic oscilloscope, that is, the TR microwave signal is obtained.

## 2.2 Theoretical Model

The essential devices in the microwave photonic TR system are two linear single-mode (SM) dispersion fibers with a length ratio of 1:2, wherein the dispersion coefficients of the two stage dispersion fibers are mutually opposite. The  $\ddot{\Phi} = Dl$  refers to the dispersion value of fiber, where  $D$  is the group velocity dispersion per unit length and  $l$  is the length of fiber.  $D = d^2k/d\omega^2$ , where  $k$  and  $\omega$  are the wave number and the angular frequency, respectively. Since a linear SM dispersion fiber only takes the second-order dispersion effect into consideration and its high-order dispersion is negligible [23], it can be mathematically modeled as a linear and time-invariant system with a quadratic phase response and unit amplitude response [24]. Passing through Fiber A, the optical pulse  $a(t)$  becomes:

$$b(t) = a(t) * \exp\left(j\frac{t^2}{2\ddot{\Phi}_1}\right) \quad (1)$$

The  $\ddot{\Phi}_1$  refers to the dispersion value of Fiber A. If  $|\ddot{\Phi}_1/\tau^2| \gg 1$ , where  $\tau$  is the pulse-width of  $a(t)$ , the Fraunhofer approximation can be adopted [25], and then Eq. (1) can be expressed as:

$$b(t) \approx \exp\left(j\frac{t^2}{2\ddot{\Phi}_1}\right) \times A(\omega) \Big|_{\omega=\frac{t}{\ddot{\Phi}_1}} \quad (2)$$

where  $A(\omega)$  is the Fourier transform of  $a(t)$ .

The synchronous microwave signal  $m(t)$ , which is received by Antenna B, is loaded onto the chirped optical pulse by the MZM, and the output signal of the MZM is:

$$c(t) = b(t) \times m(t) \quad (3)$$

Putting Eq. (2) into Eq. (3), we have

$$c(t) = \exp\left(j\frac{t^2}{2\ddot{\Phi}_1}\right) \times A(\omega) \times m(t) \Big|_{\omega=\frac{t}{\ddot{\Phi}_1}} \quad (4)$$

The modulated signal  $c(t)$  passes through Fiber B and becomes:

$$i(t) = c(t) * \exp\left(j\frac{t^2}{2\ddot{\Phi}_2}\right) \quad (5)$$

where  $\ddot{\Phi}_2$  is the dispersion value of Fiber B.

Eq. (5) can be expressed as:

$$i(t) = A(\omega) \Big|_{\omega=\frac{t}{\ddot{\Phi}_1}} \times \exp\left(j\frac{t^2}{2\ddot{\Phi}_2} - j\frac{\left(\frac{t}{2\ddot{\Phi}_2}\right)^2}{\left(\frac{1}{2\ddot{\Phi}_1} + \frac{1}{2\ddot{\Phi}_2}\right)}\right) \times \int_{-\infty}^{+\infty} m(\tau) \times \exp\left[j\left(\frac{1}{2\ddot{\Phi}_1} + \frac{1}{2\ddot{\Phi}_2}\right)\left(\tau - \frac{\frac{t}{\ddot{\Phi}_2}}{\frac{1}{\ddot{\Phi}_1} + \frac{1}{\ddot{\Phi}_2}}\right)^2\right] d\tau \quad (6)$$

Thanks to approximation of Dirac function [26]:

$$\delta(t) \approx \lim_{\ddot{\Phi}_{1,2} \rightarrow 0} \sqrt{\frac{j\pi(\ddot{\Phi}_1 + \ddot{\Phi}_2)}{\ddot{\Phi}_1\ddot{\Phi}_2}} \times \exp\left(\pm \frac{j(\ddot{\Phi}_1 + \ddot{\Phi}_2)t^2}{\ddot{\Phi}_1\ddot{\Phi}_2}\right) \quad (7)$$

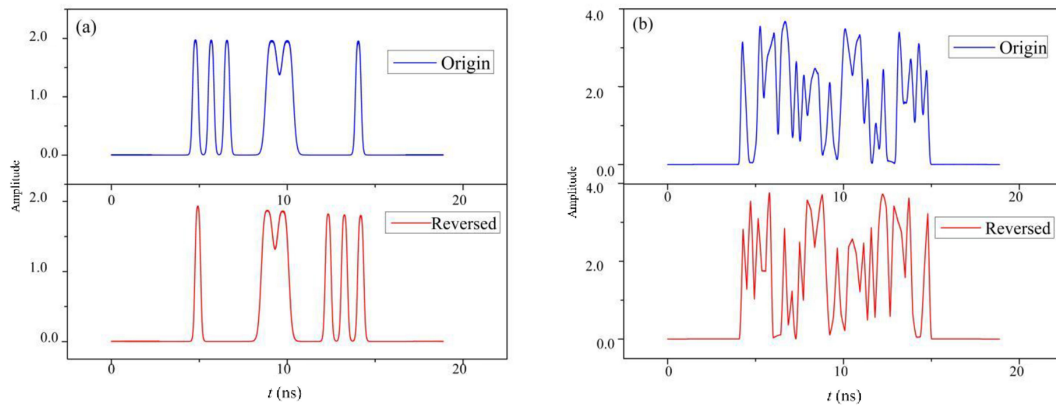


Fig. 2. Comparison of the simulation microwave signal waveforms and their corresponding reversed waveforms: (a) 3:2:1 waveform (b) arbitrary waveform.

Eq. (6) can be reduced to:

$$i(t) \approx A(\omega) \Big|_{\omega=\frac{t}{\Phi_1}} \sqrt{\frac{j\pi(\ddot{\Phi}_1\ddot{\Phi}_2)}{\ddot{\Phi}_1 + \ddot{\Phi}_2}} \exp\left(\frac{jt^2}{\ddot{\Phi}_1 + \ddot{\Phi}_2}\right) \times m\left(\frac{\ddot{\Phi}_1}{\ddot{\Phi}_1 + \ddot{\Phi}_2}t\right) \quad (8)$$

Supposing

$$2\ddot{\Phi}_1 = -\ddot{\Phi}_2 = 2\ddot{\Phi} \quad (9)$$

Eq. (8) becomes:

$$i(t) = A\left(\frac{t}{\Phi}\right) \times \sqrt{2j\pi\ddot{\Phi}} \times \exp\left(\frac{jt^2}{-\Phi}\right) \times m(-t) \quad (10)$$

We can see from Eq. (10) that the signal  $m(t)$  is time-reversed to  $m(-t)$ .  $A(t/\ddot{\Phi})$  can be seen as the spectrum of the optical pulse from the MLL after passing through the dispersion fibers. Ideally, the ultrashort optical pulse emitted from the MLL is very wide and smooth in the spectrum, which will have small effect on the microwave waveform. The distortion of microwave waveforms is mainly due to bandwidth limitation, which will be analyzed in Section 2.3.2.

### 2.3 Simulation Analysis

**2.3.1 Simulation:** Software Optisystem is used for numerical simulation to verify the TR system. As shown in Fig. 2, the 3:2:1 pulse waveform microwave signal is reversed to a 1:2:3 pulse waveform; the arbitrarily generated microwave signal is also accurately reversed.

It is observed that the microwave signals up to 10 ns are accurately reversed. The duration of the TR signal will be analyzed in Section 2.3.3.

**2.3.2 Bandwidth Limitation:** System bandwidth is an important factor affecting TR system performance. In this design of the TR experimental system, the linear SM dispersion fiber is lower in prices and has broad bandwidth. The electronic devices used such as MZM, PD and antennas, have wideband properties (10 GHz). Therefore, only the dispersion value limiting the system bandwidth needs to be considered. The relationship between the bandwidth of photonic stretch system and the dispersion value of the dispersive device was derived in [27]. In application to microwave photonic TR system, the relation is:

$$\Delta f_{3dB} = \sqrt{\frac{1}{4\pi\ddot{\Phi}}} \quad (11)$$

where  $\Delta f_{3dB}$  is the 3 dB system bandwidth,  $\ddot{\Phi}$  is the dispersion value.

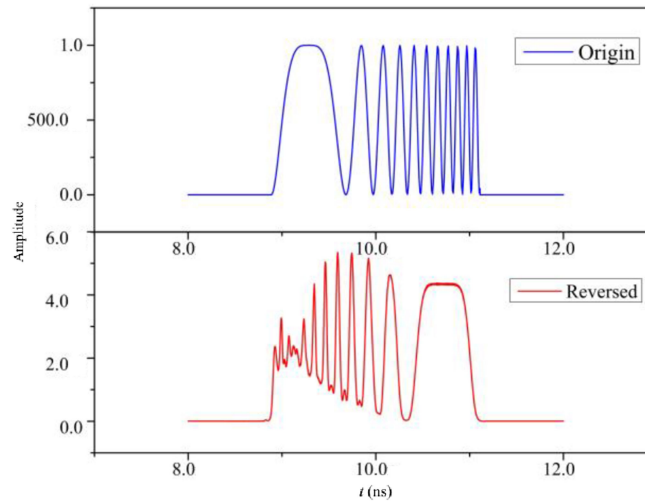


Fig. 3. Comparison of the original signal waveform and the distorted time-reversed waveform.

In order to reveal the impact of dispersion value on TR system bandwidth, we generated an input microwave signal, which is approximately regarded as a sequence of Gaussian pulses with constantly narrowing pulse width. Noticing that a Gaussian pulse with  $\tau$ -long pulse width has a  $1/(\pi\tau)$  spectrum, so when condition  $\tau < \sqrt{1/4\pi\Phi}$  is satisfied, the TR signal begins to be distorted. Fig. 3 shows the TR signal distortion caused by the system bandwidth limitation of dispersion. If continuously increasing the dispersion of the dispersive devices, the TR system performance will continue to deteriorate.

**2.3.3 Temporal Aperture Limitation:** The maximum duration of microwave signal that the TR system can reverse is defined as the temporal aperture, which depends on the dispersion value of the dispersive device and the optical pulse width emitted by the MLL [27]:

$$\tau_{3dB} = \sqrt{2 \ln 2 (\tau_0^2 + \Phi^2 \tau_0^{-2})} \quad (12)$$

When condition  $|\Phi^2/\tau_0^2| \gg 1$  is satisfied, formula (12) is reduced to:

$$\tau_{3dB} \approx \frac{\sqrt{2 \ln 2} \Phi}{\tau_0} \quad (13)$$

where  $\tau_{3dB}$  is the temporal aperture width,  $\tau_0$  denotes the half-width at  $1/e$  maximum of the pulse, and  $\Phi$  is dispersion value.

Fig. 4(a) shows the dispersion value  $\Phi$  and the temporal aperture  $\tau_{3dB}$  are proportional when  $\tau_0 = 210$  fs. Fig. 4(b) shows  $\tau_0$  and  $\tau_{3dB}$  are inversely proportional when  $\Phi = 3.91 \times 10^{-22} \text{ s}^2$ . The curve acquired from formula (13) is consistent with the simulation results. To further improve the duration of the TR signal, ultrashort pulse with narrower pulse width and dispersive device with higher dispersion coefficient are very necessary, such as replacing the MLL with one of better performance or increasing the length of dispersion fiber. However, the system bandwidth and the temporal aperture are contradictory to each other. In order to increase the duration of the TR signal and increase the dispersion value of the dispersive device, the bandwidth of the TR system is strongly limited as [18]. The pulse width of the ultrashort optical pulse emitted by the MLL cannot be less than 50fs, otherwise the high-order dispersion cannot be neglected. Therefore, it is necessary and valuable to increase the temporal aperture width without affecting the bandwidth of the TR system.

**2.3.4 Experimental Results:** According to Fig. 1, the experimental platform of microwave photonic TR system was constructed in the laboratory. The lengths of two linear SM fibers are 20 km



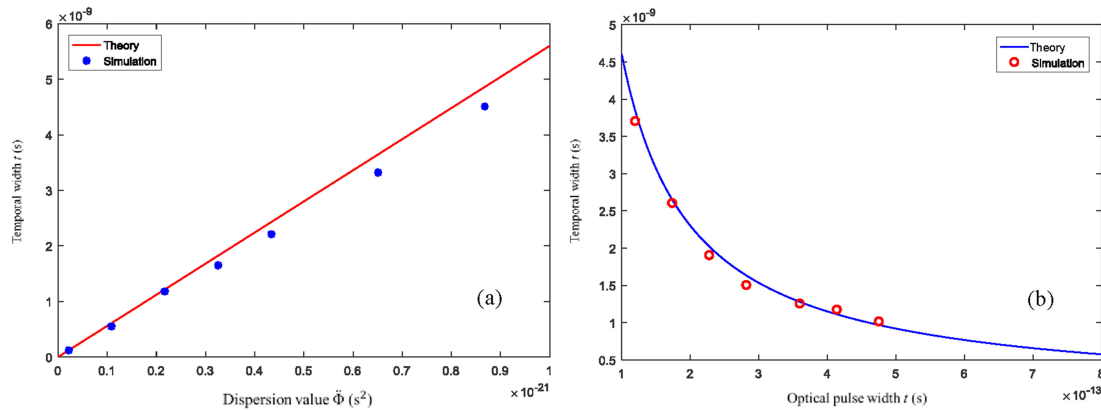


Fig. 4. Relationship between the temporal aperture width and the dispersion coefficient, the optical pulse width: (a) The temporal aperture width and the dispersion value are proportional; (b) The temporal aperture width and the optical pulse width are inversely proportional.

and 40 km and their dispersion coefficients are approximately 17 ps/nm/km and  $-17$  ps/nm/km, respectively. According to Eq. (11), the bandwidth of our system is about 14 GHz. Therefore, the system bandwidth is determined by the bandwidth of the electronic device, that is, 10 GHz. The center wavelength of the ultrashort pulse from MLL is about 1560 nm (experimental test result of the self-built MLL, there is a deviation from the central wavelength of 1550 nm, which has no effect on experimental results) with  $\tau_0$  less than 300 fs. The values of dispersion and optical pulse width are close to  $\ddot{\Phi}$  and  $\tau_0$  in the previous paragraph, so the temporal aperture is limited to approximately 1.2 ns. The repetition rate of the optical pulse train from MLL is 11.6 MHz. The OC is used to split the energy of the optical pulse with a ratio of 90:10. The AWG (Tektronix 7122B) with a sampling rate of 24 GS/s was used for the generation of microwave signal. Antenna A was connected to AWG and Antenna B received the microwave signal emitted by Antenna A. The distance between the two antennas is approximately 30 cm. Antenna B was connected to MZM (Kangguan Optoelectronics KG-AMBOX, bandwidth of 10 GHz). The microwave signal and the optical signal achieve synchronization by the trigger signal applied from the PD (Kang Guan Photoelectric KG-PT-10G, bandwidth of 10 GHz) to the AWG. The TR optical signal was detected to an electrical signal by the PD (Kang Guan Photoelectric KG-PT-10G, bandwidth of 10 GHz). Microwave signal waveform was observed in real time by an oscilloscope (Tektronix 72004B) with a bandwidth of 20 GHz. Three different waveforms of microwave signals were generated by the AWG to verify the designed TR system, as shown in Figs. 5(a)–(c). We can observe a slight change in the waveform of the TR signal. By improving the flatness of the optical carrier, it is possible to reduce the waveform variations, such as using a MLL with flatter spectrum and a fiber with more uniform dispersion coefficient distribution. Fig. 5(d) shows the spectrum of the microwave signals with three different waveforms. Microwave signals time-reversed with bandwidth up to 10 GHz have been implemented.

### 3. Prototype of TR-UWB Communication System

#### 3.1 System Configuration

In order to apply the developed TR module to UWB communication, we proposed a prototype system of TR-UWB information transmission. Fig. 6 depicts the schematic of the full analog TR-UWB communication system. In this system, we referred to the binary on-off keying (OOK) for information modulation method [1], and it is proposed to use the microwave switch to modulate the signal on/off. The AWG is connected to the first port of circulator (1) (three-port circulator, port cycle mode is 1-2-3-1), the second port of circulator (1) is connected to the transmitting antenna Port1, and the third port of circulator (1) is connected to the oscilloscope. The antenna Port2 is

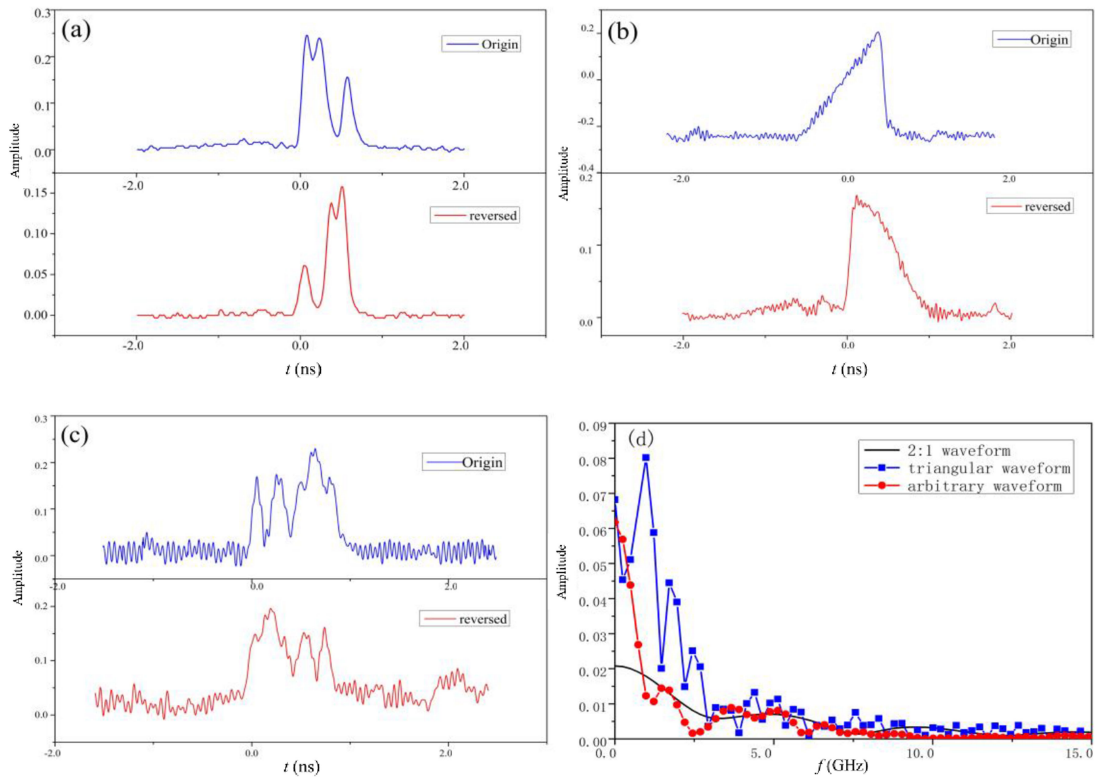


Fig. 5. Comparison of the experimental microwave signal waveforms and their corresponding reversed waveforms: (a) 2:1 waveform (b) uphill triangular waveform (c) arbitrary waveform (d) Spectrum of the experimental microwave signals.

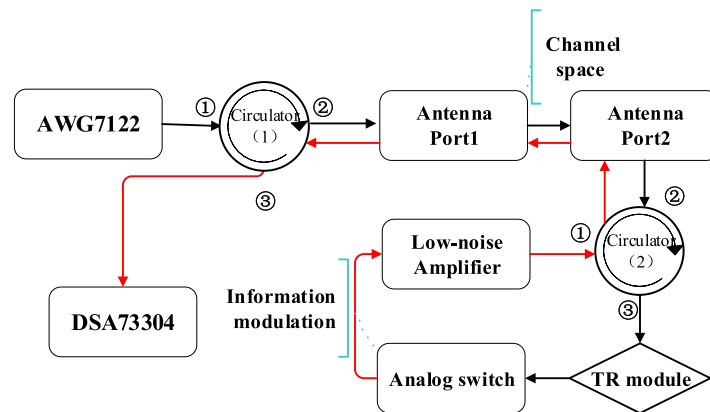


Fig. 6. Schematic of proposed TR-UWB communication system based on the demonstrated analog TR module.

connected to the second port of circulator (2) (three-port circulator, port cycle mode is 1-2-3-1), and the distance between the two antennas is about 15 cm. The third port of circulator (2) is connected to the input port of the TR module (the RF input of the MZM), and the output of the TR module (the RF output of the PD) is connected to the input of the microwave switch (Analog Devices, EV1HMC347ALP3E). The output of the switch is connected to the first port of circulator (2) through a low-noise amplifier.



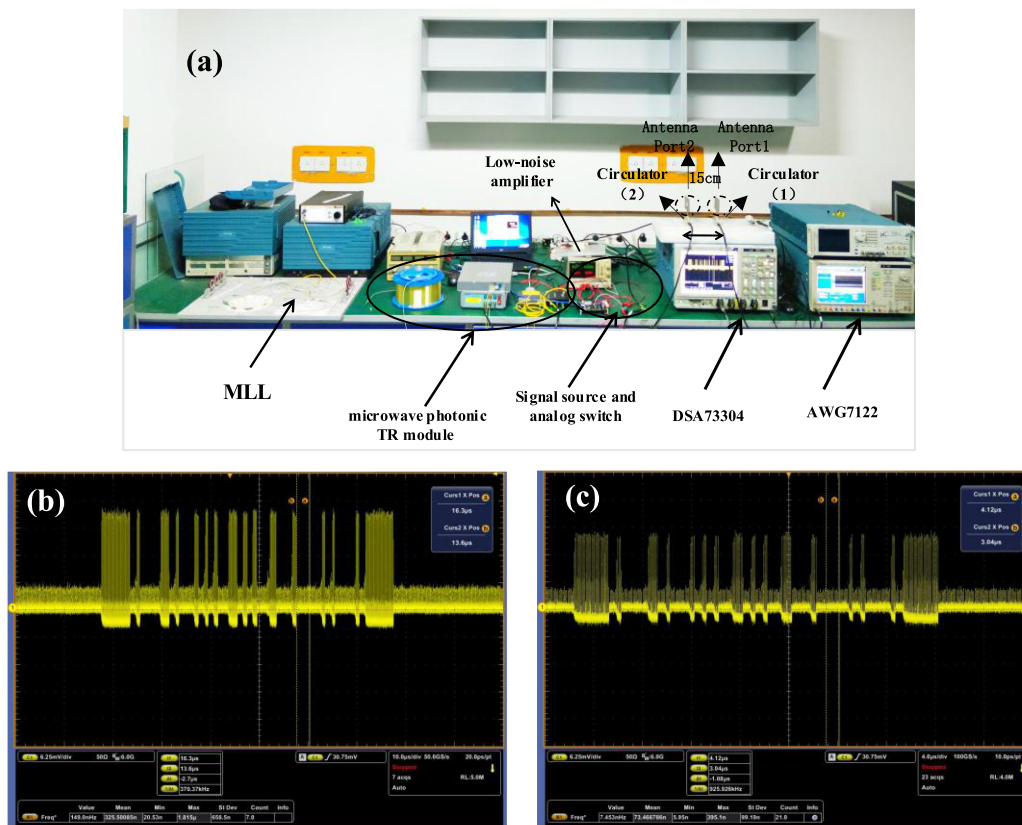


Fig. 7. The proposed full analog devices TR-UWB system and experimental test results: (a) Photograph of the TR-UWB experimental platform; (b) TR-UWB information transmission of 8-bit ASCII code with 1 Mbit/s; (c) TR-UWB information transmission of 8-bit ASCII code with 2 Mbit/s.

### 3.2 Experimental Results

A piece of letter information, “CEMLAB”, encoded with 8-bit ASCII code was used for UWB information transmission. The photograph of an experimental platform based on the schematic shown in Fig. 5 is presented in Fig. 7(a). The AWG generated repeated sounding microwave signal to be transmitted through Port1. The temporal signal bandwidth is 2–4.3 GHz, limited by the bandwidth of the circulator. After propagation in the channel space, repeated signal was received by Port2. The repeated signal passed through circulator (2) and entered the TR module. The signal passing through the microwave photonic TR module was time-reversed, and its repetition rate was consistent with MLL. The microwave switch was used to control whether the time-reversed signal was transmitted or not to modulate the information. The time-reversed signal was transmitted to represent the bit information “1”, otherwise the bit information was “0”. The switch used a complementary negative control voltage logic  $-5/0$  V operation and a FPGA chip combined with a voltage source as signal source, which generated a control signal based on the ACSII code of the information to control the switch on/off. In the actual experimental setup, since the control signal and the time-reversed signal were difficult to synchronize, we made the switching rate less than the signal repetition rate and the control signal was marked with 6 bit information “1” at the beginning and end for DSA collection. The time-reversed signal carrying the information was amplified by the low noise amplifier and entered the third port of circulator (2). It was transmitted by Port2 through the channel space and received by Port1. Therefore, we completed the information modulation, transmission and reception in real time.

The switching time was set to 1 us and 0.5 us respectively, so that the information transfer rate is 1 Mbit/s and 2 Mbit/s respectively. We collected the received signal from the oscilloscope as shown in Fig. 7(b) and Fig. 7(c). From the preliminary experimental results, we can demodulate the information and successfully restore “CEMLAB” according to the ACSII code, which indicates that the proposed TR-UWB communication system works and has potential application.

#### 4. Conclusions

In conclusion, we have constructed a broadband microwave photonics TR module and applied it into a prototype of TR-UWB communication system. The structure of the TR module was demonstrated and a theoretical model was established based on the temporal pulse shaping principle. The low-cost dispersion fibers and self-made MLL are used for temporal shaping of optical pulses, MZM and PD are used for modulation and demodulation of microwave signals. Experimental results indicate that the TR module has an excellent TR performance for microwave signals and its system bandwidth exceeds 10 GHz. The TR-UWB communication system using full analog devices was implemented to a preliminary information transmission experiment, which completely gets rid of the digital signal processing technology. Therefore, the signal detection, TR, real-time modulation and information transmission can be realized without the aid of costly high-end equipment. The experimental results verified the feasibility of this system and prove the great potential for indoor wireless communication and UWB remote sensing. These applications provide unique capabilities for high-capacity transmission and obscured-target detection using TR-UWB electromagnetic signals.

#### References

- [1] L.-Q. Yang and G. B. Giannakis, “Ultra-wideband communications: An idea whose time has come,” *IEEE Signal Process. Mag.*, vol. 21, no. 6, pp. 26–54, Nov. 2004.
- [2] G. R. Aiello and G. D. Rogerson, “Ultra-wideband wireless systems,” *IEEE Microw. Mag.*, vol. 4, no. 2, pp. 36–47, 2003.
- [3] G. Lerosey, J. De Rosny, A. Tourin, A. Derode, G. Montaldo, and M. Fink, “Time reversal of electromagnetic waves,” *Phys. Rev. Lett.*, vol. 2, no. 19, pp. 19–21, May 2004.
- [4] A.-M. Dariush and T.-T. Vahid, “Time reversal technique for ultra wideband (TR-UWB) communication systems and its performance analysis,” in *Proc. Int. Symp. Telecommun.*, 2008, pp. 219–223.
- [5] R. C. Qiu, C. Zhou, N. Guo, and J. Q. Zhang, “Time reversal with MISO for ultra-wideband communications: Experimental results,” *IEEE Antennas Wireless Propag. Lett.*, vol. 5, pp. 269–273, 2006.
- [6] F. X. Liu, B.-Z. Wang, Q. S. Xiao, and J. S. Lai, “Post-time-reversed MIMO ultrawideband transmission scheme,” *IEEE Trans. Antennas Propag.*, vol. 58, no. 5, pp. 1731–1738, May 2010.
- [7] Y. Song, T. N. Guo, R. C. Qiu, and M. C. Wicks, “A real time UWB MIMO system with programmable transmit waveforms: Architecture, algorithms and demonstrations,” *IEEE Trans. Antennas Propag.*, vol. 60, no. 8, pp. 3933–3940, Aug. 2012.
- [8] A. Dezfouliyan, S. Member, and A. M. Weiner, “Experimental investigation of UWB impulse response and time reversal technique up to 12 GHz: Omnidirectional and directional antennas,” *IEEE Trans. Antennas Propag.*, vol. 60, no. 7, pp. 3407–3415, Jul. 2012.
- [9] M. E. Yavuz and F. L. Teixeira, “Ultrawideband microwave sensing and imaging using time-reversal techniques: A review,” *Remote Sens.*, vol. 1, no. 3, pp. 466–495, 2009.
- [10] G. Lerosey, J. de Rosny, A. Tourin, A. Derode, and M. Fink, “Time reversal of wideband microwaves,” *Appl. Phys. Lett.*, vol. 88, no. 15, 2006, Art. no. 154101.
- [11] A. C. Fannjiang, “On time reversal mirrors,” *Inverse Problems*, vol. 25, no. 9, 2009, Art. no. 095010.
- [12] D. R. Jackson and D. R. Dowling, “Phase conjugation in underwater acoustics,” *J. Acoust. Soc. Amer.*, vol. 89, no. 1, pp. 171–181, 1991.
- [13] S. Sha, V. K. Shenoya, S. Jung, M. Lu, K. Min, and S. Lee, “A hardware architecture for time reversal of short impulses based on frequency domain approach,” *Proc. SPIE*, vol. 7308, no. 73, 2009, Art. no. 73080T.
- [14] H. Zhai *et al.*, “An electronic circuit system for time-reversal of ultra-wideband short impulses based on frequency-domain approach,” *IEEE Trans. Microw. Theory Techn.*, vol. 58, no. 1, pp. 74–86, Jan. 2010.
- [15] B. H. Kolner and M. Nazarathy, “Temporal imaging with a time lens,” *Opt. Lett.*, vol. 14, no. 12, pp. 630–632, 1989.
- [16] B. H. Kolner, “Space-time duality and the theory of temporal imaging,” *IEEE J. Quantum Electron.*, vol. 30, no. 8, pp. 1951–1963, Aug. 1994.
- [17] J. D. Schwartz, S. Member, J. Azaña, D. V. Plant, and S. Member, “A fully electronic system for the time magnification of ultra-wideband signals,” *IEEE Trans. Microw. Theory Techn.*, vol. 55, no. 2, pp. 327–334, Feb. 2007.
- [18] S. Ding, B.-Z. Wang, G. D. Ge, D. Wang, and D. S. Zhang, “Realization of microwave wave signal time reversal based on time lens theory,” (in Chinese), *Acta Phys. Sin.*, vol. 61, no. 6, pp. 74–86, 2012.
- [19] M. S. Liang, B.-Z. Wang, S. Ding, J. Y. Li, and Z. M. Zhang, “Time reversal of electromagnetic waves using the dispersion compensation approach,” *IEEE Photon. J.*, vol. 7, no. 4, Aug. 2015, Art. no. 6500207.

- [20] F. Coppinger, A. Bhushan, and B. Jalali, "Time reversal of broadband microwave signals," *Electron. Lett.*, vol. 35, no. 15, pp. 1230–1232, 1999.
- [21] H. Linget, L. Morvan, J.-L. Le Gouët, and A. Louchet-Chauvet, "Time reversal of optically carried radiofrequency signals in the microsecond range," *Opt. Lett.*, vol. 38, no. 5, pp. 643–645, 2013.
- [22] J. Zhang and J. Yao, "Broadband and precise microwave time reversal using a single linearly chirped fiber bragg grating," *IEEE Trans. Microw. Theory Techn.*, vol. 63, no. 7, pp. 2166–2172, Jul. 2015.
- [23] C. Wang, M. Li, and J. Yao, "Continuously tunable photonic microwave frequency multiplication by use of an unbalanced temporal pulse shaping system," *IEEE Photon. Technol. Lett.*, vol. 22, no. 17, pp. 1285–1287, Sep. 2010.
- [24] M. A. Muriel, J. Azana, and A. Carballar, "Real-time fourier transformer based on fiber gratings," *Opt. Lett.*, vol. 24, no. 1, pp. 1–3, 1999.
- [25] J. Yao, "Photonic generation of microwave arbitrary waveforms," in *Proc. 16th Opto-Electron. Commun. Conf.*, 2011, pp. 356–357.
- [26] A. Papoulis, *Signal Analysis*. New York, NY, USA: McGraw-Hill, 1977, pp. 269–278.
- [27] Y. Mei *et al.*, "Harmonics analysis of the photonic time stretch system," *Appl. Opt.*, vol. 55, no. 26, pp. 7222–7228, 2016.